

High Pressure Sensing Using Fiber Bragg Gratings Written in Birefringent Side Hole Fiber

Stephen Kreger, Sean Calvert, Eric Udd

Blue Road Research
376 NE 219th Ave
Gresham, OR 97030
Tel: 503 667 7772 Fax: 503 667 7880

Abstract

Pressure measurements are made by measuring Bragg grating peak splitting caused by transverse strain differences in the core of a single mode side hole fiber. The side holes and not the fiber exterior are pressurized, demonstrating the ability to use the side holes as a pressure conduit so that pressure measurements can be made in a thermally and mechanically stable environment. Geometrical and residual stress-based birefringence stemming from partial side hole collapse during the drawing process allows measurements to be made near atmospheric pressures. Peak fitting techniques are used to determine peak separation to sub-pm levels despite substantial peak overlap.

Introduction

Fiber optic pressure sensors have attracted attention in recent years because they are passive, immune to electromagnetic interference, intrinsically safe, multiplexible and corrosion resistant. These advantages make them good candidates for high range pressure sensing in hostile environments. Fiber Bragg grating sensors are intrinsically sensitive to both strain and temperature, and thus are useful for making simultaneous measurements of temperature and pressure-induced strain. Traditional Bragg grating sensors based on axial strain, however, are plagued by high temperature and pressure cross-sensitivity. Previous work with Bragg gratings in single mode side hole fiber used the difference in transverse strains to measure pressure up to 12 kpsi and temperature up to 300 C with relatively low cross-sensitivity.^{1,2} These efforts, however, neglected the difficulty of measuring lower pressures when the peaks corresponding to strain in orthogonal directions overlapped, or fell directly on top of each other. However, this problem can be overcome by making side hole fiber with intrinsic geometrical or stress birefringence.^{3,4} We produce side hole fiber with a small amount of geometrical and stress birefringence by using the tendency of the side holes to partially collapse during the preform draw step used to produce side hole fiber with an elliptical core. The resulting peak separation of 77 pm (at 1550 nm), along with the development of curve fitting techniques to determine the separation of two identical overlapping peaks allow us to make pressure measurements in a range starting at atmospheric pressures.

Modeling

The Bragg grating peak center separation $\lambda_x - \lambda_y$ generated by difference in transverse strains $\epsilon_x - \epsilon_y$ in the fiber core is given by:

$$\frac{\lambda_x - \lambda_y}{\lambda_o} = \frac{n_o^2}{2} (p_{12} - p_{11}) (\epsilon_x - \epsilon_y). \quad (1)$$

In the above equation p_{ij} are components of the strain-optic tensor, n_o is the effective index of the mode propagating in the core, and λ_o is the center wavelength of the grating in the unstrained state. For a typical germanosilicate optical fiber $p_{12} = 0.252$, $p_{11} = 0.113$, and $n_o = 1.46$.⁵ Thus the peak separation is typically given by

$$\frac{\lambda_x - \lambda_y}{\lambda_o} = 0.148 (\epsilon_x - \epsilon_y). \quad (2)$$

Finite element analysis software was used to predict the strain difference for various side hole geometries. Figure 1 shows typical results for the case in which the side holes are pressurized and the exterior of the fiber remains at atmospheric pressure. For the case in which the exterior of the fiber is pressurized and the side holes remain at atmospheric pressure the strain values are the same, but the signs are reversed. The maximum equivalent stress is experienced at the edge of the side holes closest to the fiber core. Figure 2 shows the transverse strain difference at

the core as a function of side hole size for three separate side hole separations. Core transverse strain differences increase nearly linearly with hole size and distance from the core. However, core size and outer wall thickness requirements place limits on practical side hole size and separation.

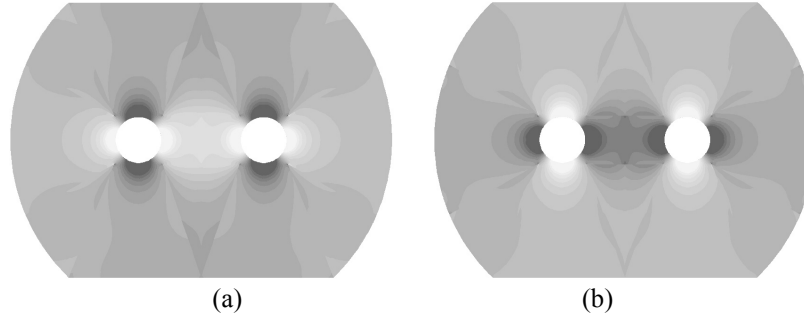


Figure 1. Strain contour plots for fiber with flattened sides and 15 μm hole diameters spaced 26 μm apart along the x axis. The strain range is + 50 $\mu\text{m}/\text{m}$ for black and - 50 $\mu\text{m}/\text{m}$ for white for 1000 psi side hole pressure. At the fiber core strain a) in the x direction is compressive, and b) in the y direction is tensile.

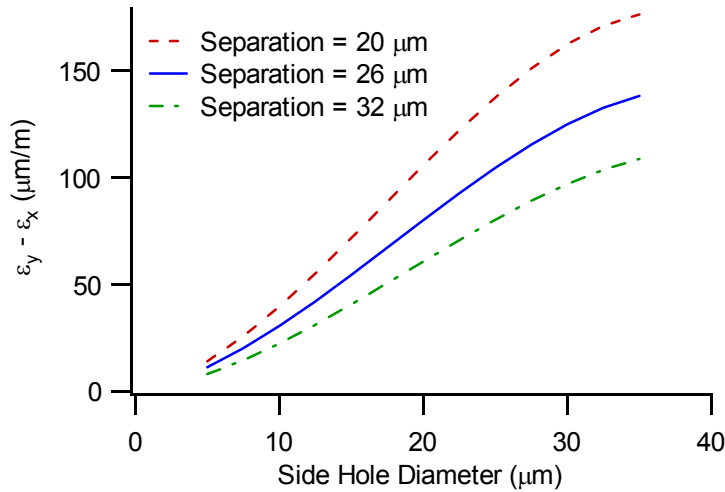


Figure 2. Core transverse strain difference as a function of side hole size for three side hole separations, for side hole pressure of 1000 psi.

Experiment

Flats were milled and holes were drilled into a preform designed to exhibit performance characteristics similar to Corning SMF 28. The flats provide a geometrical reference outside the fiber and aid in low contact point stress positioning and alignment. The preform was drawn at a high enough temperature so that the holes partially collapsed, resulting in 15 μm diameter holes 26 μm apart and an elliptical core with major and minor axis length of 14 and 8 μm . Cross sections of the resulting fiber are shown in Figure 3. The fiber is single mode despite the core ellipticity and bend loss was below 3 dB when the fiber was looped in a circle of 8 mm diameter. The fiber was hydrogen loaded and unapodized Bragg gratings with center wavelength close to 1550 nm and a full width at half maximum of close to 200 pm were written into the fiber. None of the gratings failed the subsequent 1.5% axial strain proof test. Epoxy acrylate was used for both the original coating and recoating after grating application. The side hole fiber was cleaved at approximately 8 cm from the grating and epoxied into a small hole drilled into the end of a pressure fitting such that only 3 cm of the fiber extended into the pressure tube as shown in figure 4. The fiber was fusion spliced to a SMF-28 patch cable on the other side of the grating to plug the side holes.

The grating was illuminated with a broadband Er^{3+} fiber source, and a 30 dB extinction polarizer was used in series with a polarization controller to illuminate each grating peak. The spectral intensity data for each peak was curve fitted to the functional form for the reflectivity of a Bragg grating with constant period and modulation amplitude as

derived from coupled mode theory:⁶

$$R(\lambda) = \frac{\Omega^2 \sinh^2(sl)}{\Delta k^2 \sinh^2(sl) + s^2 \cosh^2(sl)} \quad (3)$$

The index perturbation coupling coefficient Ω is given by $\Omega = \pi \Delta n M_p / \lambda_B$, the detuning wave vector Δk is given by $\Delta k = 2\pi n_0 (1/\lambda - 1/\lambda_B)$, λ_B is the Bragg center wavelength $\lambda_B = 2n_0 \Lambda$, and the parameter s is defined by $s^2 = \Omega^2 - \Delta k^2$, where Λ is the grating period, l is the grating length, Δn is the difference between core and cladding indices, n_0 is the effective mode index, and M_p is the fraction of the mode power contained by the fiber core. The spectral intensity data and curve fits for the peaks are displayed in Figure 5. The values determined by the curve fit are $\Omega = 0.3597e-6$ 1/nm, $l = 7.963$ mm, $\lambda_{B1} = 1549.8139$ nm, and $\lambda_{B2} = 1549.8911$ nm.

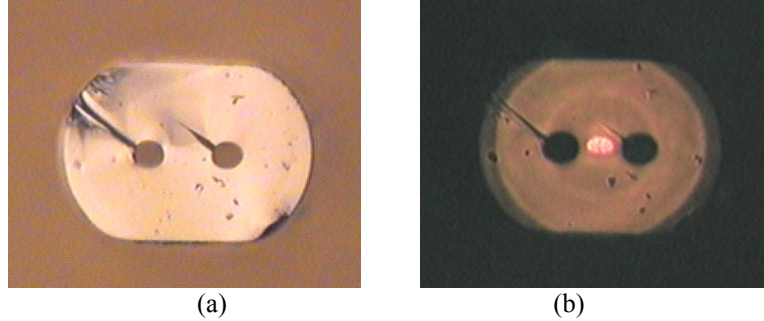


Figure 3. Custom fiber with flats and side holes a) illuminated in reflection, b) illuminated in transmission using a fiber coupled white light source.

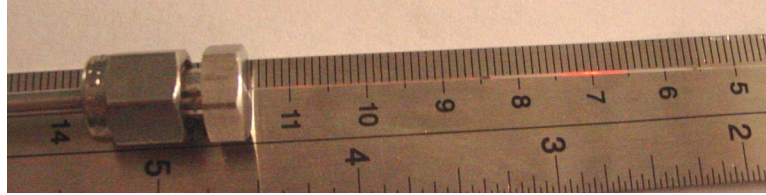


FIGURE 4. Side hole fiber epoxied in a hole drilled in a pressure tube cap. A red light fault finder is used to illuminate the grating.

The polarizer and polarization controller were removed so that the grating was illuminated by the unpolarized broadband fiber source. Spectral intensity waveforms were collected over a pressure range of 0 to 5000 psi using a gas bottle regulator to vary pressure, and the previous values for Ω and l were used to fit the data to a new function similar to Equation 3 which assumed the presence of two identical but wavelength shifted peaks. Examples of the data collected and the resulting curve fits at 0 and 5000 psi are depicted in Figure 6. Increasing pressure causes the strain difference $\epsilon_x - \epsilon_y$ to decrease, thus canceling some of the intrinsic birefringence and causing the peaks to move together. Note, however, that the peak width of the two waveforms varies considerably with peak level due to the effects of the overlapping side lobes. The resulting peak separation response to pressure is shown in Figure 7. The gas regulator gauge only had a resolution of 50 psi, but the peak separation measurements were stable and repeatable to 0.1 pm. Given the slope of the response curve, it is likely that the resolution is limited by the gas regulator and not the peak separation determination. The curve nonlinearity is also likely due to the gas regulator gauge and not the side hole fiber response as previous studies showed linearity over a much larger strain range. Pressure tests will be repeated with a more accurate and stable pressure controller in the near future.

Summary

We have demonstrated pressure measurements using Bragg gratings in intrinsically birefringent side hole fiber for the first time, enabling pressure measurements to be made near atmospheric pressures. We also demonstrated the feasibility of using peak curve fitting techniques to determine peak separation with a resolution of 0.1 pm even when there is substantial peak overlap. These sensors also exhibit the intrinsic low temperature cross sensitivity and small size of previous Bragg grating side hole sensors compared to axial strain based Bragg grating pressure sensors.

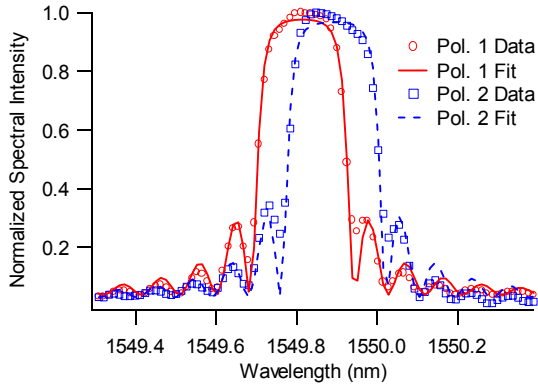


Figure 5. Spectral waveforms of the two overlapping peaks recorded one polarization at a time and the resulting curve fits to Equation 3.

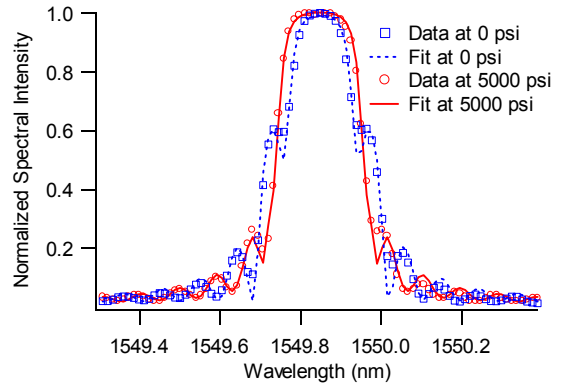


Figure 6. Unpolarized spectral waveforms and resulting curve fits of the overlapping peaks taken at 0 and 5000 psi.

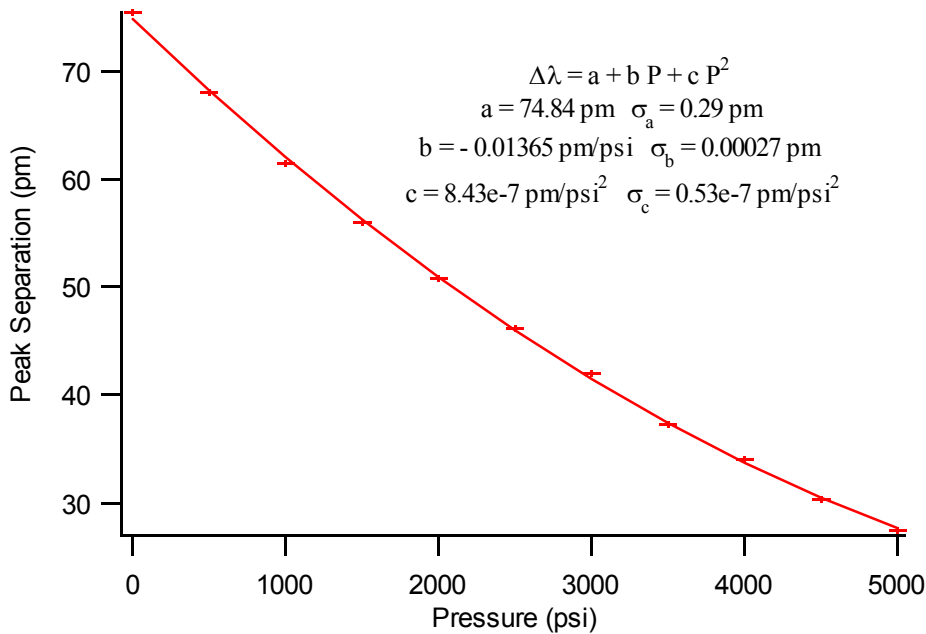


Figure 7. Peak separation response to pressure.

References

1. R. J. Schroeder, T. Yamate, and E. Udd, "High Pressure and Temperature Sensing in the Oil Industry Using Fiber Bragg Gratings Written onto side hole Single Mode Fiber," OFS-13, SPIE Vol. 3746, pp. 42-45, 1999.
2. T. Yamate, R.T. Ramos, R.J. Schroeder, E. Udd, "Thermally Insensitive Pressure Measurements up to 300 degree C using Fiber Bragg Gratings Written onto Side Hole Single Mode Fiber," SPIE Proceedings, Vol. 4185, pp. 628-630, 2000.
3. J. Wojcik, P. Mergo, M. Makara, "Anomaly of Sensitivity to Pressure of Side-Hole HB Optical Fiber," SPIE Proceedings, Vol. 3730, pp. 2-7 1998.
4. J. Wojcik, W. Urbanszyk, W. Bock, B. Janoszczyk, P. Mergo, M. Makara, K. Poturaj, W. Spytek, "Prototype of the Side-Hole HB Optical Fiber," SPIE Proceedings, Vol. 3731, pp. 88-93, 1998.
5. R. B. Wagreich, W. A. Atia, H. Singh, and J. S. Sirkis, "Effects of Diametrical Load on Fiber Bragg Gratings Fabricated in Low Birefringent Fiber," Electronics Letters, vol. 32, pp. 1223-1224, 1996.
6. Lam, D. K. W., and B. K. Garside, "Characterization of single mode optical fiber filters," Applied Optics, Vol. 20, 1981, pp. 440-445.